

The whistle and the rattle: The design of sound producing muscles

(rattlesnake/toadfish/calcium transients/muscle mechanics/swimbladder)

LAWRENCE C. ROME*†‡, DOUGLAS A. SYME*, STEPHEN HOLLINGWORTH§, STAN L. LINDSTEDT¶,
AND STEPHEN M. BAYLOR§

Departments of *Biology and §Physiology, University of Pennsylvania, Philadelphia, PA 19104; †Marine Biological Laboratories, Woods Hole, MA 02543; and ‡Department of Biological Sciences, Northern Arizona University, Flagstaff, AZ 86011

Communicated by Clara Franzini-Armstrong, University of Pennsylvania School of Medicine, Philadelphia, PA, April 15, 1996
(received for review December 11, 1995)

ABSTRACT Vertebrate sound producing muscles often operate at frequencies exceeding 100 Hz, making them the fastest vertebrate muscles. Like other vertebrate muscle, these sonic muscles are “synchronous,” necessitating that calcium be released and resequestered by the sarcoplasmic reticulum during each contraction cycle. Thus to operate at such high frequencies, vertebrate sonic muscles require extreme adaptations. We have found that to generate the “boatwhistle” mating call (≈ 200 Hz), the swimbladder muscle fibers of toadfish have evolved (i) a large and very fast calcium transient, (ii) a fast crossbridge detachment rate, and (iii) probably a fast kinetic off-rate of Ca^{2+} from troponin. The fibers of the shaker muscle of rattlesnakes have independently evolved similar traits, permitting tail rattling at ≈ 90 Hz.

Skeletal muscle fibers perform a wide range of activities, and different fiber types are accordingly designed to operate at different speeds and frequencies (1). A number of modifications appear to underlie this diversity. For example, in locomotory muscle, compared with slow twitch fibers, fast twitch fibers have a faster myosin with a higher maximum velocity of shortening (V_{\max}) (2, 3), a greater content of sarcoplasmic reticulum (SR), and its associated Ca^{2+} pumps (4, 5), a different isoform of the SR Ca^{2+} pump (SERCA1 in fast versus SERCA2 in slow) (6, 7) and a greater concentration of parvalbumin (a soluble protein that binds both calcium and magnesium) (5, 8). There is also evidence that fast fibers have a briefer myoplasmic free Ca^{2+} concentration ($[\text{Ca}^{2+}]$) transient (9, 10) and less sensitive force–pCa relationship (11, 12).

To understand the physiological modifications that underlie very rapid contractions, we have studied two of the fastest vertebrate muscles known. Both of these “sonic” muscles are used to produce sounds at the frequency at which the muscle contracts. The “boatwhistle” mating call of the male toadfish (*Opsanus tau*) is generated by ≈ 200 Hz contractions (25°C) of the muscles encircling the fish’s gas-filled swimbladder (13–15). The familiar “rattle” of the venomous western diamond-back rattlesnake (*Crotalus atrox*) is generated by ≈ 90 Hz contractions (35°C) of the shaker muscles at the base of the tail (16–19). The operational frequencies of these sonic muscles are 1–2 orders of magnitude higher than those of the locomotory muscles in the same animals (0.5–5 Hz) (20).

For fibers to operate at such high frequencies, they must activate and relax rapidly. Based on morphological and biochemical evidence from swimbladder of a very large SR Ca^{2+} pump density, a high density of SR Ca^{2+} release sites, and a large parvalbumin concentration, it has been proposed that an important modification of these sonic fibers is unusually rapid Ca^{2+} cycling (5, 21). By measuring myoplasmic free $[\text{Ca}^{2+}]$, we found that these fibers do indeed have unusual Ca^{2+} tran-

sients—in fact the largest and fastest ever recorded. However, our results showed that a fast Ca^{2+} transient alone is not sufficient for high frequency operation. By measuring V_{\max} , an index of crossbridge detachment rate, and the force–pCa relationship in skinned fibers, a possible index of troponin kinetics, we found that rapid activation and relaxation likely also require a modification of the crossbridge kinetic rate, and probably a modification of the kinetics of Ca^{2+} –troponin binding. In reaching these conclusions, we first compared the above measurements in three fiber types from toadfish, ranging from slow twitch swimming fibers to the superfast twitch swimbladder fibers. We then compared the properties of rattlesnake shaker fibers with those of swimbladder.

MATERIALS AND METHODS

In toadfish, the anatomical segregation of different fiber types permitted us to dissect small bundles of fibers (pure in fiber type) from the slow twitch red and fast twitch white trunk musculature, and the superfast twitch swimbladder muscles. In rattlesnakes, small fiber bundles were dissected from shaker muscle, which is also composed of a single fiber type (18). Fiber bundles were mounted in one of three chambers for different physiological measurements.

Myoplasmic $[\text{Ca}^{2+}]$ Transient. The change of myoplasmic free $[\text{Ca}^{2+}]$ was monitored during contractions by using furaptra, a fluorescent calcium indicator with rapid reaction kinetics (22). The delay between a change in $[\text{Ca}^{2+}]$ and a change in furaptra’s fluorescence is not likely to be more than 0.2 ms (23). Furaptra was pressure injected into a single fiber within a small bundle, and experiments and calibration were performed as in ref. 22. The fluorescence transients from swimbladder fibers were corrected for a small, Mg^{2+} -dependent delayed decrease in fluorescence due to the exchange of Ca^{2+} for Mg^{2+} on parvalbumin (22). Additionally, in the case of swimbladder fibers, a correction to furaptra’s resting fluorescence was made to account for the fraction (0.28) of indicator molecules located in the central core of the fiber (5), where the change in $[\text{Ca}^{2+}]$ during a brief period of stimulation is likely to be negligible. To reduce tension and thus motion artifacts, fibers were stretched to sarcomere lengths (SL) of 2.7–3.0 μm (swimbladder) and 3.3–4.0 μm (other fiber types). Action potentials were initiated with point stimulation, and fibers were studied only if they responded in all-or-none fashion.

Muscle Mechanics. Muscle force was measured in all experimental setups by means of a force transducer attached to one end of a fiber bundle. In the muscle mechanics setup, the other end of the bundle was attached to a servomotor that imposed length changes on the muscle bundle. Bundles were

excited by field stimulation. The force–velocity curves of the red and white toadfish fibers were determined by using force clamp measurements (24). The force–velocity curves of the rattlesnake shaker fibers were determined by using length ramps (24). In all cases, V_{\max} was obtained by extrapolating the curve to zero force. For the swimbladder, V_{\max} was most accurately determined by using the slack test (24). Previous comparisons of these different techniques on other fiber types show that they all give the same V_{\max} (24); thus the results can be compared directly.

The workloop technique (25, 26) was also used to determine if the muscle could generate mechanical work at high oscillation frequencies. In this method, the muscle length was changed sinusoidally and the timing of the single stimulus during the length cycle was adjusted to maximize power output.

Force–pCa Measurements. The force generated by “skinned” (permeablized) fibers was measured as a function of free $[Ca^{2+}]$, which was set with a Ca^{2+} /EGTA buffer system (27). The solutions had a pH of 7.1 (15°C) and ionic strength of 200 mM; the experiments were conducted at a SL of 2.2–2.3

μm . The preparation was adjusted for the size of the fibers: for toadfish red muscle, single fibers were used; for toadfish white and frog muscles, single fibers were split longitudinally to $\approx 1/4$ of their diameter; for swimbladder muscle, bundles of two or three fibers were used. Skinned fibers from rattlesnakes proved unstable, and only the threshold for force generation could be determined. Preparations were skinned in 3% Triton X-100 for 20 min and then exposed to 10 μM thapsigargin (an SR calcium pump blocker) throughout the experiments. Both treatments abolish SR Ca^{2+} pumping, thereby preventing the SR from interfering with the measurements.

Modeling. Ca^{2+} binding to troponin at 16°C was modeled from the Ca^{2+} transient (as in ref. 28) with several different values assumed for k_{off} (the Ca^{2+} off-rate constant from troponin). Fractional troponin activation (equivalent to $[\text{troponin occupancy}]^2$) was estimated under the assumptions that (i) there are two equal and independent binding sites for Ca^{2+} , having a k_{on} for Ca^{2+} binding of $0.9 \times 10^8 \text{ M}^{-1}\cdot\text{s}^{-1}$, and (ii) both sites must be occupied to generate force. The relative rates of SR Ca^{2+} pumping in different fiber types of toadfish were estimated from the Ca^{2+} transient as in ref. 28.

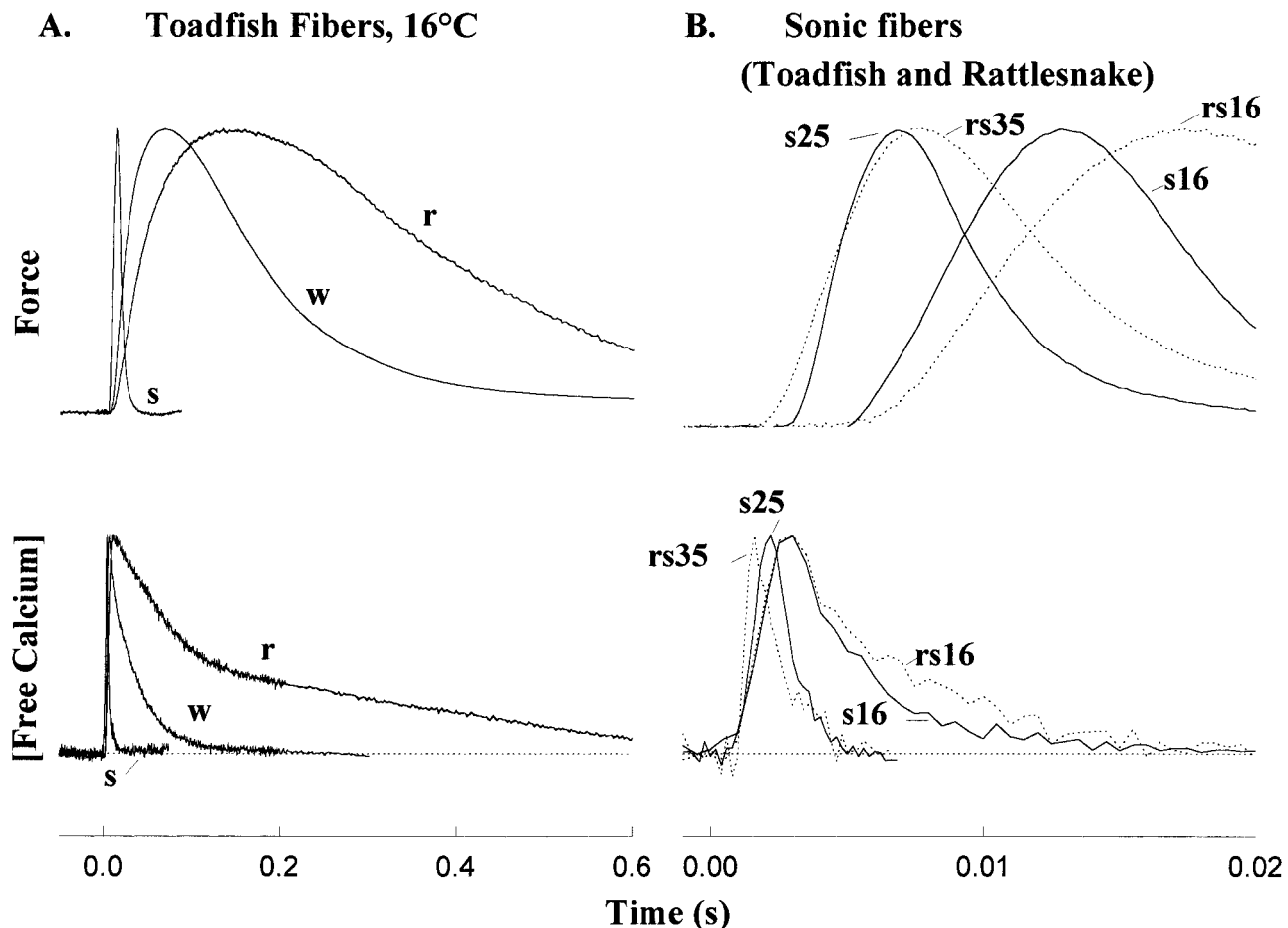


FIG. 1. Twitch tension (*Upper*) and calcium transients (*Lower*) of three fiber types from toadfish at 16°C (*A*) and of sonic fibers at 16–35°C (*B*). In each case, the force and the calcium transient have been normalized to their maximum value. (*A*) The twitch and calcium transient become briefer going from the slow-twitch red fiber (*r*), to the fast-twitch white fiber (*w*), and to the superfast-twitch swimbladder fiber (*s*). (*B*) Records from rattlesnake shaker fibers (*rs*; dotted line) at 16°C and swimbladder fibers (*s*; solid line) at 16°C and 25°C. The average (\pm SE) peak magnitudes of the calcium transients were as follows: $7.0 \pm 1.2 \mu\text{M}$, $n = 3$ (*r*); $11 \mu\text{M}$, $n = 1$ (*w*); $50.7 \pm 3.6 \mu\text{M}$, $n = 5$ (*s16*); $27 \pm 5 \mu\text{M}$, $n = 2$ (*s25*); $8.9 \pm 1.3 \mu\text{M}$, $n = 3$ (*rs16*); $8.4 \pm 1.9 \mu\text{M}$, $n = 3$ (*rs35*). The average half-widths of the Ca^{2+} transients were as follows: $110 \pm 49 \text{ ms}$ (*r*); 21 ms (*w*); $3.4 \pm 0.1 \text{ ms}$ (*s16*); $1.5 \pm 0.1 \text{ ms}$ (*s25*); $4.4 \pm 0.2 \text{ ms}$ (*rs16*); $1.5 \pm 0.2 \text{ ms}$ (*rs35*). The average half-widths of twitch tension were as follows: $516 \pm 56 \text{ ms}$, $n = 5$ (*r*); $79 \pm 7 \text{ ms}$, $n = 6$ (*w*); $9.5 \pm 0.2 \text{ ms}$, $n = 7$ (*s16*); $5.8 \pm 0.2 \text{ ms}$, $n = 2$ (*s25*); $25.7 \pm 3.5 \text{ ms}$, $n = 4$ (*rs16*); $8.5 \pm 1.5 \text{ ms}$, $n = 4$ (*rs35*). All swimbladder values are for the longer first twitch (see Fig. 2). Note that the time scale is expanded about 30-fold in *B*. Note also that in Figs. 1 and 2, the force records shown for the swimbladder and shaker fibers were made on the mechanics apparatus because field stimulation overcame action potential conduction delays in the fibers. The swimbladder force traces are from experiments performed at a SL of 2.3 μm (the SL at which the force–pCa and force–velocity relationships were also measured). At 2.7 μm , the most common SL for swimbladder Ca^{2+} measurements, the force records had similar kinetics, but poor signal-to-noise ratio because of the low active force and very high resting force.

RESULTS AND DISCUSSION

The twitch times of different fiber types in toadfish varied by about 50-fold. At 16°C, the slow-twitch red muscle (used for steady swimming at 1–2 Hz) has a twitch half-width of about 500 ms, compared with ≈ 100 ms for fast-twitch white muscle (used for burst swimming at ≈ 5 Hz), and 10 ms for the superfast swimbladder muscle (Fig. 1*A*). These dramatic differences are reflected in the tension response to repetitive stimulation. During repetitive stimulation, fusion of tetanic force occurred in the red muscle at 5–10 Hz and in the white muscle at 10–15 Hz. Clearly, these locomotory fibers could not be used for high frequency sound production because, if they surrounded the swimbladder and were stimulated at high frequencies, the resultant fused tetanus would simply compress the bladder and prevent it from vibrating. By contrast, swimbladder fibers do not show complete fusion of force until 150–200 Hz at 16°C and 250–300 Hz at 25°C.

For a fiber to activate and relax rapidly, two conditions must be met. First, myoplasmic free $[Ca^{2+}]$, the trigger for muscle contraction, must rise rapidly to a level sufficient to activate troponin, and then rapidly fall. Second, myosin crossbridges

must attach to actin and generate force soon after $[Ca^{2+}]$ rises and then detach and stop generating force soon after $[Ca^{2+}]$ falls.

To test for the first condition, we measured the change in myoplasmic $[Ca^{2+}]$ during contractions. In swimbladder fibers, the half-width of the calcium transient (3–4 ms at 16°C; Fig. 1), is the fastest ever measured for any fiber type (2–3 times faster than that of the fast twitch fiber of the frog) (22). The magnitude of the calcium transient, 30–60 μM , is also the largest ever measured [3–5 times that of a frog fiber (22)]. The importance of the calcium transient duration in setting the twitch duration can be seen in Fig. 1*A*, which shows that in going from the slow red fibers to the super-fast swimbladder fibers, both durations sped up in parallel by ≈ 50 -fold.

The significance of a fast Ca^{2+} transient is best illustrated during repetitive stimulation. During stimulation of slow red muscle at a modest 3.5 Hz (Fig. 2*A*), the decay of the calcium transient is so slow that $[Ca^{2+}]$ does not have time to return to baseline between stimuli. Even the lowest $[Ca^{2+}]$ during the contraction is above the threshold required for force generation in this fiber type (determined from Fig. 4*A*), and therefore the relaxation of force between stimuli is incomplete, resulting in a partially fused tetanus. By contrast, the swimbladder's

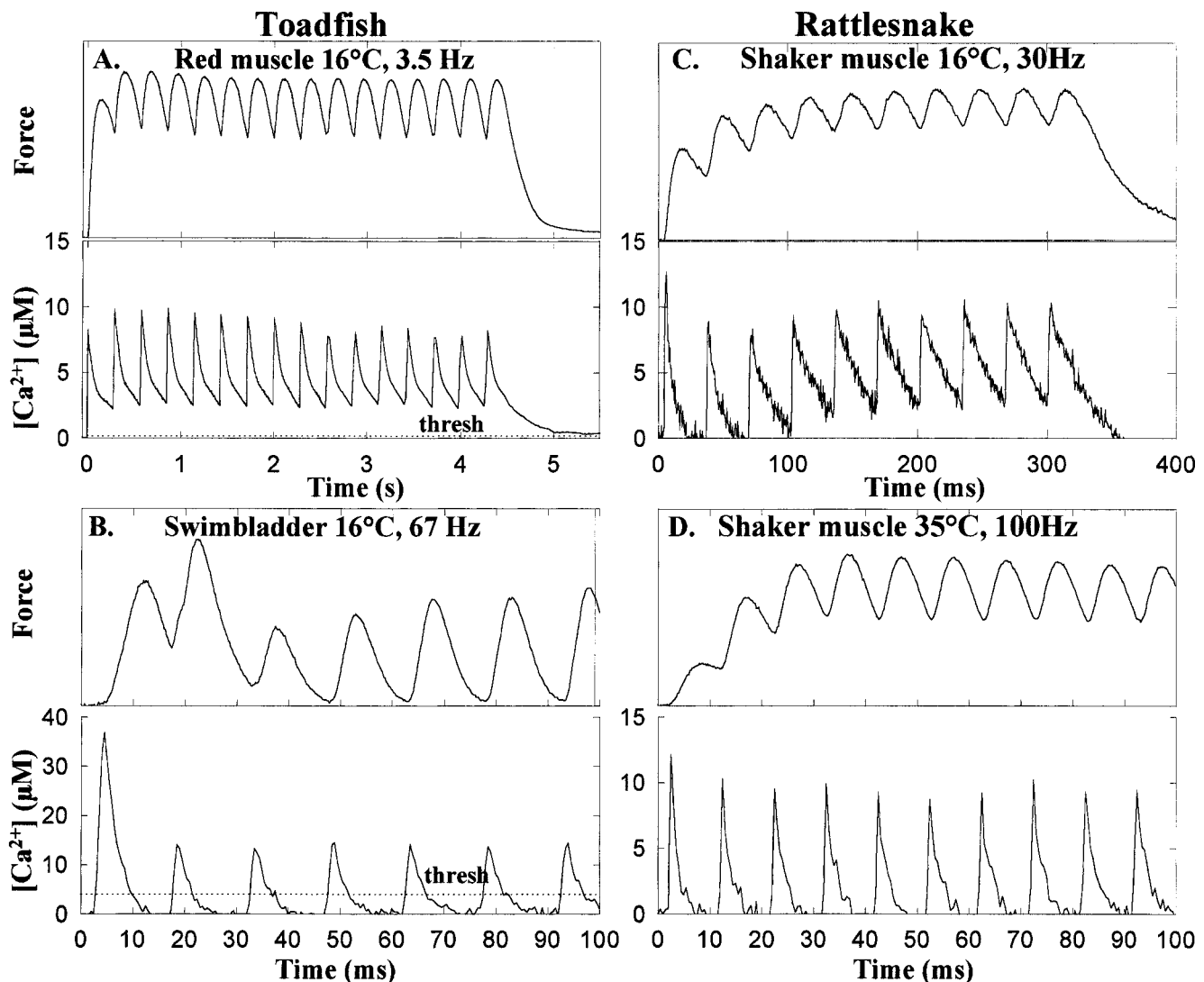


FIG. 2. Force production and calcium transients during repetitive stimuli. (A) Slow twitch red fiber stimulated at 3.5 Hz. The threshold $[Ca^{2+}]$ for force generation was derived from Fig. 4*A* and is shown with a dotted line. (B) Swimbladder fiber stimulated at 67 Hz. Note that the threshold is much higher for the swimbladder than for the red fiber; also note the different scale for the ordinate. Note also the large magnitude of the first swimbladder Ca^{2+} transient compared with subsequent ones and that the first twitch of the train has a longer duration (half-width is ≈ 10 ms) than subsequent ones (half-width is ≈ 6 ms). Both toadfish fiber experiments were performed at 16°C. (C) Rattlesnake shaker fibers at 16°C stimulated at 30 Hz. (D) Shaker fibers at 35°C stimulated at 100 Hz. Calcium thresholds are not reported for shaker fibers.

calcium transient is so rapid that even with 67 Hz stimulation, $[Ca^{2+}]$ returns easily to baseline between stimuli (Fig. 2B). In addition, except for the first twitch, $[Ca^{2+}]$ is below the threshold for force generation more than half of the time. Hence, the Ca^{2+} transient is sufficiently rapid to permit the oscillation in force required for sound production.

Even though $[Ca^{2+}]$ returns rapidly to baseline, the swimbladder fiber could not relax quickly unless its troponin rapidly released bound Ca^{2+} . Indeed, kinetic modeling (Fig. 3, trace b) indicates that if the swimbladder troponin had the off-rate for calcium (k_{off}) estimated to apply to fast twitch fibers of frog ($115\ s^{-1}$) (28), then occupancy of its troponin sites with Ca^{2+} would not decline sufficiently rapidly to permit the observed rapid and nearly complete fall in force (Fig. 3, trace a). To assess possible adaptations in the Ca^{2+} -troponin control system, the force-pCa relationship was measured (Fig. 4A). As expected, a right shift (decreased Ca^{2+} sensitivity) was found in the curves for the white fibers with respect to the red fibers, and an even lower Ca^{2+} sensitivity was found for the super-fast fibers. Based on the 3-fold right shift of the force-pCa curve of swimbladder fibers with respect to frog fibers (Fig. 4A), these results suggest that k_{off} of swimbladder troponin is 3 times faster than that of frog. [The alternative, that the presumed increased dissociation constant of the Ca-troponin reaction, $K_D (=k_{off}/k_{on})$, is the result of a smaller k_{on} , would slow the rate of force generation and thus be antithetical to high frequency operation of swimbladder fibers.] With this higher k_{off} , the modeled rate of troponin deactivation no longer appears limiting (Fig. 3, trace c). Thus the underlying benefit of the less sensitive troponin may be the possibility of faster relaxation through a more rapid k_{off} . Direct measurements of k_{off} (29) from troponin bound to thin filaments are necessary to verify this analysis. Another potential benefit of a lower affinity troponin is that, during relaxation, Ca^{2+} will dissociate from troponin at a higher $[Ca^{2+}]$; this might give rise to a steeper $[Ca^{2+}]$ gradient and faster diffusion of Ca^{2+} to the SR. The lower affinity troponin, however, requires a larger myoplasmic $[Ca^{2+}]$ for it to become saturated, and this requirement is likely related to the large magnitude of the Ca^{2+} transient observed for the swimbladder.

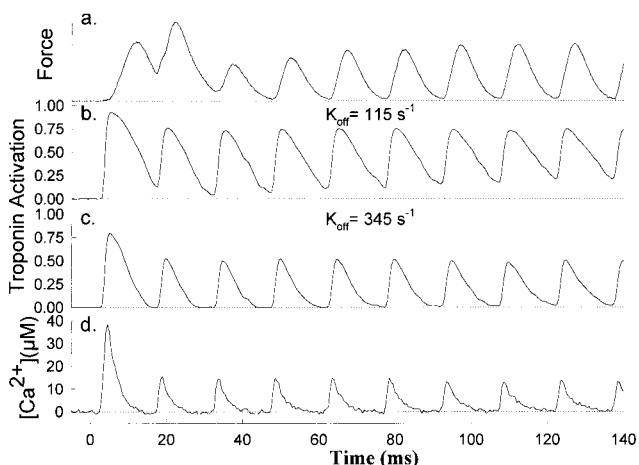


FIG. 3. Calcium transient and modeled troponin activation (see *Materials and Methods*) for a swimbladder fiber based on two different values of k_{off} . Troponin activation, so calculated, depends only on the time course of $[Ca^{2+}]$, the k_{on} and the k_{off} . A fiber was stimulated at 67 Hz and the measured Ca^{2+} transient is shown as trace d. For k_{off} to be consistent with the force record in trace a, the troponin activation (traces b and c) must decline faster than the force record, as a delay associated with crossbridge kinetics is also expected. In trace c, we assume that the ≈ 0.5 log unit (≈ 3 -fold) right shift in the pCa_{50} between frog (5.71) versus toadfish swimbladder (5.23) (see Fig. 4A) is the result of a 3-fold faster k_{off} (345 versus $115\ s^{-1}$).

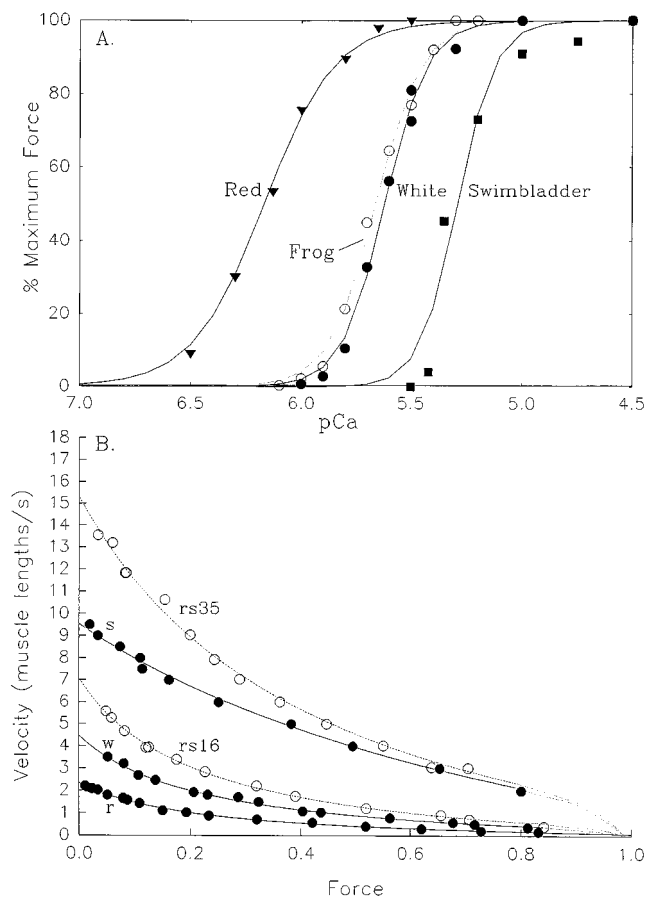


FIG. 4. (A) Force-pCa relationship of a toadfish red, white, and swimbladder fiber and a frog (*Rana temporaria*) fiber at $16^\circ C$. For each fiber type an individual force-pCa ($-\log[Ca^{2+}]$) data set is shown along with a curve fitted using the equation: $\% Force = [100 \cdot (10^{-pCa})^N] / [(10^{-pCa})^N + (10^{-pCa_{50}})^N]$. The mean pCa_{50} values of the red, white, and swimbladder fibers were 6.30 ± 0.08 , $n = 4$; 5.63 ± 0.03 , $n = 4$; and 5.23 ± 0.04 , $n = 4$, respectively. Frog fibers had a mean pCa_{50} of 5.71 ± 0.03 , $n = 3$. Note that the force from swimbladder fibers rose more sharply than the fitted curve at forces below 50% and more gradually at forces above 80%. (B) Force-velocity curves of toadfish and rattlesnake fibers. For each fiber type an individual force-velocity data set is shown. The corresponding unconstrained Hill equation (20) is fitted up to 80% isometric force (solid or dashed line), beyond which the curve is approximated with a spline fit (dotted line). The force-velocity curves of the toadfish red (r) and white (w) and swimbladder fibers are shown with solid symbols and lines. Note that the swimbladder (s) V_{max} was determined from the slack test and its force-velocity curve is shown only for comparison. The force-velocity curves of the rattlesnake shaker fibers (rs) are shown with open symbols and dashed curves. The mean values for V_{max} in muscle lengths (ML) per s were as follows: red (2.43 ± 0.04 , $n = 4$), white (4.12 ± 0.29 , $n = 4$), swimbladder (11.8 ± 0.8 , $n = 5$), shaker at $16^\circ C$ (7.68 ± 1.78 , $n = 4$), and shaker at $35^\circ C$, (18.3 ± 2.3 , $n = 3$). All toadfish measurements were at $16^\circ C$.

Finally, for force to drop quickly following the dissociation of Ca^{2+} from troponin, a fast crossbridge detachment rate is required. V_{max} is thought to be proportional to the crossbridge detachment rate (30). Indeed, the V_{max} of swimbladder muscle (≈ 12 ML/s) is nearly twice the speed of other fast twitch fibers at 15 - $16^\circ C$ [e.g., frog and lizard (31, 32)]. It is also 5- and 2.5-fold faster than toadfish red and white muscle, respectively (Fig. 4B), indicating a faster crossbridge detachment rate.

Our toadfish experiments have thus identified a number of kinetic variables that change progressively as twitch speed increases from the slow twitch of red fibers to the superfast twitch of swimbladder fibers. (i) The duration of the calcium

transient becomes shorter, which in turn requires more rapid calcium release and reuptake. Ultrastructural and biochemical studies suggest that this is achieved by a large increase in the density of SR calcium pumps (SERCA1 isoform), an increased concentration of parvalbumin and a short diffusion distance for Ca^{2+} ($\approx 0.15 \mu\text{m}$) in the narrow, lamellar-shaped myofibrils (5, 7, 21, 33). There is also an increase in the density of SR Ca^{2+} release channels in swimbladder fibers (5) and it has been proposed that the channel isoform in this fiber type, the α -ryanodine receptor, abbreviates the time course of Ca^{2+} release (34). The much larger increase in Ca^{2+} pump density compared with that of Ca^{2+} release sites (5) might lead to a small magnitude Ca^{2+} transient. If so, the resulting incomplete binding to troponin and incomplete activation might play a role in the very high frequency operation. Our measurements, however, show that the Ca^{2+} transient is in fact very large and sufficient to saturate troponin. (ii) Troponin has a faster off-rate for Ca^{2+} , which likely requires molecular modification of troponin to a lower affinity type (Fig. 4A). (iii) Crossbridges detach more rapidly (Fig. 4B), which likely involves molecular modification of myosin.

Most importantly, changes in all of these parameters in concert enable swimbladder fibers to perform the mechanical work necessary to produce sound energy at high frequencies. Workloop experiments, which test the ability of fibers to generate net positive work under steady oscillatory conditions, show that swimbladder fibers can perform work at frequencies in excess of 200 Hz (25°C; Fig. 5A), representing the highest frequency for work production ever recorded in vertebrate muscle. By contrast, locomotory muscles lack the combination of fast relaxation and high V_{max} necessary to generate work at these high frequencies. For instance, the highest frequency for vertebrate locomotory muscles is an order of magnitude lower, 25–30 Hz [mouse (35) and lizard (36) fast-twitch muscles at 35°C].

With these physiological design principles in place, we then examined the rattlesnake shaker muscle to determine whether this sonic muscle independently evolved similar traits. At 16°C, the shaker fibers have a very rapid calcium transient (half-width = 4–5 ms), which is only 1–2 ms slower than that of the

swimbladder (Fig. 1B Lower). However, the shaker muscle twitch half-width is considerably longer (25 versus 10 ms) than that of swimbladder (Fig. 1B Upper). This slower twitch likely reflects the effects of slower crossbridge detachment (its V_{max} of $\approx 7 \text{ ML s}^{-1}$ is only about half that of the swimbladder; Fig. 4B) and possibly a slower troponin k_{off} (because the threshold $[\text{Ca}^{2+}]$ for force generation $\{\text{pCa} = 5.98 \pm 0.07, n = 3\}$, is similar to frog fibers and thus lower than swimbladder fibers). Although hypertrophy of the SR has led to the hypothesis that a primary adaptation for sonic muscles is a fast Ca^{2+} transient, this analysis suggests that in fact *all* three systems must be very rapid to produce the fastest contractions. Thus at 16°C, shaker fibers can be stimulated up to only ≈ 20 Hz before summation of force begins (30 Hz is the rattling frequency at 16°C) (Fig. 2C) and fusion occurs at ≈ 50 Hz.

At 35°C, where snakes rattle at 90 Hz, the calcium transient (Fig. 1B) and the V_{max} (Fig. 4B) are even faster than for the swimbladder muscle at 16°C. In addition, k_{off} has a high temperature dependence (J. D. Johnson, personal communication) and thus is likely very rapid as well. The resulting briefer twitch (half-width = 8–9 ms) enables the shaker fibers to be stimulated at 100 Hz without complete fusion of force (Fig. 2D) and to perform work at 90 Hz (Fig. 5B). The similarity of the modifications in this sound producing muscle to those in toadfish is suggestive of convergent evolution, which supports the hypothesis that these modifications are necessary for high frequency direct-coupled sound production by synchronous muscle. Remarkably, in the swimbladder muscle, rapid kinetics in each step of relaxation is achieved at low temperatures, whereas in the shaker muscle, the requisite rapid kinetics can only be achieved by the accelerating effects of high temperature.

Finally, it is important to recognize that muscles with a brief activation–relaxation cycle require a potential increase in the volume of the SR and mitochondria, which reduces the space available for the force-generating myofilaments (18, 21, 37). Modeling from our $[\text{Ca}^{2+}]$ transients suggests that the rate of Ca^{2+} pumping at their respective *in vivo* operating frequencies is about 50-fold greater in the swimbladder than in the red muscle, in agreement with the large fraction of the swimbladder fiber volume (≈ 0.3) allocated to SR (5). As first suggested by previous investigators (18, 21, 37), if a fast muscle is to be used continuously and therefore aerobically (e.g., as is the case for shaker muscle), a large volume of mitochondria is required to generate ATP to fuel this high rate of Ca^{2+} pumping, further displacing the myofibrils. Clearly, a frequency limit will be reached where the reduced volume of myofibrils will not be sufficient to generate the high mechanical power required for an activity such as locomotion. For insect flight muscle, this limit is thought to be about 100 Hz (35–45°C) (38–40). To power flight at wing-beat frequencies greater than 100 Hz, insects have evolved asynchronous muscle in which a single release of calcium permits many contraction–relaxation cycles. By avoiding the large space requirements for rapid calcium cycling, more space in the asynchronous muscles can be allotted to myofibrils (37) and mitochondria (required to fuel the crossbridges), thus permitting the sustainable, high power production required for flight. Vertebrate sonic muscles, such as the toadfish swimbladder fibers as well as some insect sonic muscles (37, 41, 42), are capable of synchronous operation at frequencies well above 100 Hz. This is possible presumably because the sounds produced do not require the muscle fibers to generate mechanical power that is both high and sustained.

We gratefully acknowledge useful discussions with M. Fine, J. Crawford, C. Franzini-Armstrong, L. Sweeney, and A. Dunham. D. G. Stephenson and R. E. Godt provided advice on skinned fiber experiments. R. K. Josephson and T. A. McMahon suggested that low affinity troponin might speed diffusion. This research was supported by grants from the National Institutes of Health (L.C.R. and S.M.B.),

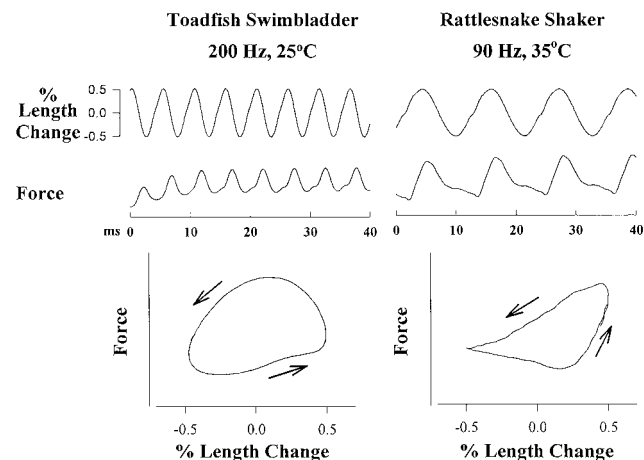


FIG. 5. Work production from a bundle of swimbladder fibers operating at 200 Hz at 25°C (A) and a bundle of rattlesnake shaker fibers operating at 90 Hz at 35°C (B). The oscillation frequencies are those at which the muscles are used *in vivo* at these temperatures. We used a strain of $\pm 0.5\%$ for both fiber types. The timing of the stimulus with respect to the length change was adjusted to maximize work production. For each fiber type, the top trace is the muscle length record and the middle trace is force production. The bottom plot is the force versus length graph of one cycle, the area of which the net work is performed during that cycle. The arrows indicate that the muscle is shortening while force is high and is being lengthened while force is low. Hence the muscle is generating positive work (25, 26).

the National Science Foundation (L.C.R. and S.L.L.), and Medical Research Council of Canada Postdoctoral Fellowship (D.A.S.).

1. Rome, L. C. & Lindstedt, S. L. (1996) in *Handbook of Physiology: Comparative Physiology*, ed. Dantzler, W. H. (Am. Physiol. Soc, Bethesda, MD), in press.
2. Reiser, P. J., Moss, R. L., Giulian, G. & Greaser, M. L. (1985) *J. Biol. Chem.* **260**, 9077–9080.
3. Sweeney, H. L., Kushmerick, M. J., Mabuchi, K., Streter, F. A. & Gergely, J. (1988) *J. Biol. Chem.* **263**, 9034–9039.
4. Ferguson, D. G. & Franzini-Armstrong, C. (1988) *Muscle Nerve* **11**, 561–570.
5. Appelt, D., Shen, V. & Franzini-Armstrong, C. (1991) *J. Muscle Res. Cell Motil.* **12**, 543–552.
6. Lytton, J., Westlin, M., Burk, S. E., Shull, G. E. & MacLennan, D. H. (1992) *J. Biol. Chem.* **267**, 14483–14489.
7. Tullis, A. & Block, B. A. (1996) *Am. J. Physiol.*, in press.
8. Heizman, C. W., Bechtold, M. W. & Rowleson, A. M. (1982) *Proc. Natl. Acad. Sci. USA* **79**, 7243–7247.
9. Eusebi, F., Miledi, R. & Takahasi, T. (1985) *Biomed. Res.* **6**, 129–138.
10. Caroll, S., Klein M. G. & Schneider, M. F. (1995) *Biophys. J.* **68**, 177a (abstr.).
11. Kerrick, W. G. L., Secrist, D., Coby, R. & Lucas S. (1976) *Nature (London)* **260**, 440–441.
12. Stephenson, D. G. & Williams, D. A. (1981) *J. Physiol. (London)* **317**, 281–302.
13. Skoglund, C. R. (1961) *J. Biophys. Biochem. Cytol.* **10**, 187–200.
14. Fine, M. L. (1978) *Oecologia* **36**, 45–57.
15. Bass, A. B. & Baker, R. (1991) *Brain Behav. Evol.* **37**, 1–15.
16. Chadwick, L. E. & Rahn, H. (1954) *Science* **119**, 442–443.
17. Martin, J. H. & Bagby, R. M. (1972) *Copeia* **3**, 482–485.
18. Schaeffer P., Conley, K. E. & Lindstedt, S. L. (1996) *J. Exp. Biol.* **199**, 351–358.
19. Martin, J. H. & Bagby, R. M. (1972) *Exp. Zool.* **185**, 293–300.
20. Secor, S., Jayne, B. & Bennett, A. F. (1992) *J. Exp. Biol.* **163**, 1–14.
21. Block, B. A. (1994) *Annu. Rev. Physiol.* **56**, 535–577.
22. Konishi, M., Hollingworth, S., Harkins, A. B. & Baylor, S. M. (1991) *J. Gen. Physiol.* **97**, 271–301.
23. Zhao M., Hollingworth, S. & Baylor, S. M. (1996) *Biophys. J.* **70**, 896–916.
24. Julian, F. J., Rome, L. C., Stephenson, D. G. & Striz, S. (1986) *J. Physiol. (London)* **370**, 181–199.
25. Josephson, R. K. (1985) *J. Exp. Biol.* **114**, 493–512.
26. Rome, L. C. Swank, D. & Corda, D. (1993) *Science* **261**, 340–343.
27. Julian, F. J., Rome, L. C., Stephenson, D. G. & Striz, S. (1986) *J. Physiol. (London)* **380**, 257–273.
28. Baylor, S. M., Chandler, W. K. & Marshall, M. W. (1983) *J. Physiol. (London)* **344**, 625–666.
29. Johnson, J. D., Nakkula, R. B., Vasulka, C. & Smillie, L. B. (1994) *J. Biol. Chem.* **269**, 8919–8923.
30. Huxley, A. F. (1957) *Prog. Biophys. Chem.* **7**, 255–318.
31. Renaud, J. M. & Stevens, E. D. (1984) *J. Exp. Biol.* **108**, 57–75.
32. Marsh, R. L. & Bennett, A. F. (1986) *J. Exp. Biol.* **126**, 63–77.
33. Fine, M. L., Bernard, B. & Harris, T. (1993) *Can. J. Zool.* **71**, 2262–2274.
34. O'Brien, J., Meissner, G. & Block, B. (1993) *Biophys. J.* **65**, 1–10.
35. James, R. S., Altringham, J. D. & Goldspink, D. F. (1995) *J. Exp. Biol.* **198**, 491–502.
36. Swoap, S. J., Johnson, T. P., Josephson, R. K. & Bennett, A. F. (1993) *J. Exp. Biol.* **174**, 185–197.
37. Josephson, R. K. & Young, D. (1981) *Am. Zool.* **27**, 991–1000.
38. Pringle, J. W. S. (1949) *J. Physiol. (London)* **108**, 226–232.
39. Smith, D. S. (1983) *Nature (London)* **303**, 503–540.
40. Sparrow, J. C. (1995) *Nature (London)* **374**, 592–593.
41. Young, D. & Josephson, R. K. (1985) *Nature (London)* **309**, 286–287.
42. Josephson, R. K. & Young, D. (1985) *J. Exp. Biol.* **118**, 185–208.